A Time-Splitting Spectral Method for Three-Wave Interactions in Media with Competing Quadratic and Cubic Nonlinearities

Weizhu Bao[1],[*] and Chunxiong Zheng[2]

[1] *Department of Mathematics, National University of Singapore, Singapore 117543.*
[2] *Department of Mathematical Sciences, Tsinghua University, Beijing, 100084, P.R. China.*

Abstract. This paper introduces an extension of the time-splitting spectral (TSSP) method for solving a general model of three-wave optical interactions, which typically arises from nonlinear optics, when the transmission media has competing quadratic and cubic nonlinearities. The key idea is to formulate the terms related to quadratic and cubic nonlinearities into a Hermitian matrix in a proper way, which allows us to develop an explicit and unconditionally stable numerical method for the problem. Furthermore, the method is spectral accurate in transverse coordinates and second-order accurate in propagation direction, is time reversible and time transverse invariant, and conserves the total wave energy (or power or the norm of the solutions) in discretized level. Numerical examples are presented to demonstrate the efficiency and high resolution of the method. Finally the method is applied to study dynamics and interactions between three-wave solitons and continuous waves in media with competing quadratic and cubic nonlinearities in one dimension (1D) and 2D.

Key words: Nonlinear optics; three-wave; time-splitting spectral method; energy; continuous wave; soliton.

1   Introduction

In nonlinear optics, based on the model for the type-II [11] second-harmonic-generating (SHG) systems and the one for the co-propagation of two orthogonal linear polarizations

[*]Correspondence to: Weizhu Bao, Department of Mathematics, National University of Singapore, Singapore 117543. Email: bao@cz3.nus.edu.sg

in the lossless Kerr medium [9], a general model of three-wave optical interactions system, which combines the quadratic and cubic nonlinearities and birefringence, can be formulated as follows [9, 11, 12]:

$$iu_z + \frac{1}{2}\Delta u + \alpha v^* w + \gamma_1 \left(\frac{1}{4}|u|^2 + \frac{1}{6}|v|^2 + 2|w|^2\right) u + \frac{\gamma_1}{12} v^2 u^* + \gamma_2 |w|^2 v + bu = 0, \quad (1.1)$$

$$iv_z + \frac{1}{2}\Delta v + \alpha u^* w + \gamma_1 \left(\frac{1}{4}|v|^2 + \frac{1}{6}|u|^2 + 2|w|^2\right) v + \frac{\gamma_1}{12} u^2 v^* + \gamma_2 |w|^2 u - bv = 0, \quad (1.2)$$

$$2iw_z + \frac{1}{2}\Delta w + \alpha uv + 2\gamma_1 \left(2|w|^2 + |u|^2 + |v|^2\right) w + \gamma_2(uv^* + u^*v)w - qw = 0, \quad (1.3)$$

where $u = u(\mathbf{x}, z)$, $v = v(\mathbf{x}, z)$ and $w = w(\mathbf{x}, z)$ are complex-valued functions, the fields u and v are complex envelopes of the two components with fundamental frequency, w is that of the single second harmonic component, and f^* is the complex conjugate of a function f. For the parameters in (1.1)-(1.3), b is a real birefringence coefficient, q is the phase-mismatch parameter that controls the SHG process, α is the coefficient for quadratic nonlinearity, and γ_1 and γ_2 are coefficients for cubic nonlinearities. All these parameters are real, and they may be positive or negative, with a constraint that γ_1 and γ_2 have the same sign. The cases $\gamma_1, \gamma_2 > 0$, and resp. $\gamma_1, \gamma_2 < 0$, correspond to the self-focusing and self-defocusing cubic nonlinearities.

The system (1.1)-(1.3) is written for the paraxial evolution in the *spatial domain*, so that $z \geq 0$ is the propagation distance, $\mathbf{x} \in \mathbb{R}^d$ $(d = 1, 2)$ is the transverse coordinate in the corresponding planar waveguide, and the Δ operator accounts for transverse coordinates. Furthermore, it conserves a dynamical invariant (power, alias the norm of the solution, in the temporal domain, it would be wave energy), i.e.,

$$
\begin{aligned}
E(z) &= \int_{\mathbb{R}^d} \left[|u(\mathbf{x}, z)|^2 + |v(\mathbf{x}, z)|^2 + 4|w(\mathbf{x}, z)|^2\right] d\mathbf{x} \equiv \int_{\mathbb{R}^d} \left[|u(\mathbf{x}, 0)|^2 + |v(\mathbf{x}, 0)|^2 + 4|w(\mathbf{x}, 0)|^2\right] d\mathbf{x} \\
&= E(0), \quad z \geq 0.
\end{aligned}
\tag{1.4}
$$

In addition, the system also conserves the momentum and Hamiltonian, which will not be explicitly used in this work.

The general form of (1.1)-(1.3) covers many three-wave interactions in nonlinear optics. For example, when $\gamma_1 = \gamma_2 = 0$, i.e. all the cubic nonlinear terms are dropped, it is reduced to the so-called type-II SHG system which is a subject that has been studied in detail theoretically and experimentally, see reviews [11, 15]. In this case, the material birefringence is employed to phase-match two orthogonal linearly polarized components of the fundamental-frequency wave to a single second-harmonic component. In addition, if $b = 0$ and $u = v$, it is further simplified to a two-wave setting, i.e. type-I SHG system without walk-off between harmonic waves [13]. The solutions of this simplified two-wave SHG system have been analyzed by many authors, both in the 1D case and in a more

general 2D case (see page 104 in [11] for a thorough review). When $\alpha = 0$, i.e. all the quadratic nonlinear terms are dropped, it is reduced to coupled nonlinear Schrödinger equations with cubic nonlinearities arising from wave interactions in Kerr medium [3, 18] or Bose-Einstein condensation [4, 7].

There has been some recent studies which deal with the analysis and numerical solutions of the three-wave system (1.1)-(1.3). Most work was focused on the finding of the soliton solutions and the exploring of their stability property and interacting behavior [15]. By using a Crank-Nicolson finite-difference scheme, Baboiu and Stegeman [1, 2] studied the interaction between two optical soliton beams during type-I SHG in quadratic nonlinear materials, i.e. $\gamma_1 = \gamma_2 = 0$ in (1.1)-(1.3), and they found that the interaction is highly sensitive to the relative phase difference and the soliton oscillations occur during excitation between the launched beams. Etrich et al. [15] considered the collision behavior of self-trapped optical beams in quadratic nonlinear media and they found that above a critical velocity, the solitary waves behave similarly to the true solitons, while below that threshold, they merge and form oscillating states. Recently, Chen, Kaup and Malomed [12] studied three-wave solitons and continuous waves in the system (1.1)-(1.3) analytically and numerically. They found several types of solitons in the system by means of the variational approximation and numerical methods, investigated stability of the solitons by means of the Vakhitov-Kolokolov criterion and direct simulations, and studied the existence and stability of continuous-wave solutions.

Due to the fully nonlinearities and complicated wave interaction patterns in (1.1)-(1.3), an efficient and accurate numerical method is one of the key issues in studying wave dynamics and interaction in the system. Currently there are two types of numerical methods proposed in the literature for solving (1.1)-(1.3): one is the Crank-Nicolson finite-difference scheme [15] and the other one is the leap-frog pesudospectral method [12]. There are some drawbacks of the two numerical methods: the former is implicit and only second-order accurate in space and the latter is explicit but there is a severe stability constraint. Historically, time-splitting methods are among the most popular methods for studying the dynamics of Schrödinger-type equations (see earlier studies by [8, 16–19] and references therein and recent applications by [3–6]). The aim of this paper is to design a time-splitting spectral methods for the system (1.1)-(1.3). The key idea in designing our novel numerical scheme is to formulate the terms related to quadratic and cubic nonlinearities into a Hermitian matrix in a proper way. Compared with the scheme used in [12, 15], the remarkable advantage is that our scheme is unconditionally stable and time transverse invariant, and conserves the total energy in discretized level.

The paper is organized as follows. In Section 2, we propose a time-splitting spectral method for discretizing the system (1.1)-(1.3). In Section 3, we study the properties of our new numerical method and test its accuracy. It is then applied to study dynamics and wave interaction of the three-wave system in 1D and 2D in Section 4. Finally, some conclusions are drawn in Section 5.

2   A time-splitting spectral method

In order to use some standard techniques [3,5,18], by changing of variables, $w \to w/2$ and $z \to t$, we can reformulate the system (1.1)-(1.3) as

$$iu_t + \frac{1}{2}\Delta u + \frac{\alpha}{2}v^*w + \gamma_1\left(\frac{1}{4}|u|^2 + \frac{1}{6}|v|^2 + \frac{1}{2}|w|^2\right)u + \frac{\gamma_1}{12}v^2u^* + \frac{\gamma_2}{4}|w|^2v + bu = 0, \quad (2.1)$$

$$iv_t + \frac{1}{2}\Delta v + \frac{\alpha}{2}u^*w + \gamma_1\left(\frac{1}{4}|v|^2 + \frac{1}{6}|u|^2 + \frac{1}{2}|w|^2\right)v + \frac{\gamma_1}{12}u^2v^* + \frac{\gamma_2}{4}|w|^2u - bv = 0, \quad (2.2)$$

$$iw_t + \frac{1}{4}\Delta w + \alpha uv + \gamma_1\left(\frac{1}{2}|w|^2 + |u|^2 + |v|^2\right)w + \frac{\gamma_2}{2}(uv^* + u^*v)w - \frac{q}{2}w = 0. \quad (2.3)$$

For simplicity of notation, we shall introduce the method in one transverse coordinate. Generalization to two transverse coordinates is straightforward for tensor product grids and the results remain valid without modifications. In the practical implementation, we truncate the system (2.1)-(2.3) with one transverse coordinate to one defined on the interval $[a,b]$

$$iu_t + \frac{1}{2}u_{xx} + \frac{\alpha}{2}v^*w + \gamma_1\left(\frac{1}{4}|u|^2 + \frac{1}{6}|v|^2 + \frac{1}{2}|w|^2\right)u + \frac{\gamma_1}{12}v^2u^* + \frac{\gamma_2}{4}|w|^2v + bu = 0, \quad (2.4)$$

$$iv_t + \frac{1}{2}v_{xx} + \frac{\alpha}{2}u^*w + \gamma_1\left(\frac{1}{4}|v|^2 + \frac{1}{6}|u|^2 + \frac{1}{2}|w|^2\right)v + \frac{\gamma_1}{12}u^2v^* + \frac{\gamma_2}{4}|w|^2u - bv = 0, \quad (2.5)$$

$$iw_t + \frac{1}{4}w_{xx} + \alpha uv + \gamma_1\left(\frac{1}{2}|w|^2 + |u|^2 + |v|^2\right)w + \frac{\gamma_2}{2}(uv^* + u^*v)w - \frac{q}{2}w = 0, \quad (2.6)$$

which is solved with periodic boundary conditions

$$u(x,t=0) = u_0(x), \quad v(x,t=0) = z_0(x), \quad w(x,t=0) = w_0(x), \quad a \le x \le b, \quad (2.7)$$

$$u(a,t) = u(b,t), \qquad u_x(a,t) = u_x(b,t), \qquad v(a,t) = v(b,t), \quad (2.8)$$

$$v_x(a,t) = v_x(b,t), \qquad w(a,t) = w(b,t), \qquad w_x(a,t) = w_x(b,t), \quad t \ge 0, \quad (2.9)$$

where $|a|$ and $|b|$ are chosen sufficiently large so as to assure that the effect of domain truncation remains insignificant. The use of more sophisticated radiation boundary conditions is an interesting topic that remains to be examined in the future. In the system (2.4)-(2.9), it conserves the total wave energy

$$E(t) = \int_a^b \left[|u(x,t)|^2 + |v(x,t)|^2 + |w(x,t)|^2\right]\,dx \equiv \int_a^b \left[|u_0(x)|^2 + |v_0(x)|^2 + |w_0(x)|^2\right]\,d\mathbf{x}$$
$$= E(0), \qquad t \ge 0. \quad (2.10)$$

W. Bao and C. Zheng / Commun. Comput. Phys., **2** (2007), pp. 123-140

127

We choose the spatial mesh size $h > 0$ with $h = (b-a)/M$ for M an even positive integer, time step size $k > 0$ and let the grid points and time steps be

$$x_j := a + jh, \quad t_n := nk, \quad j = 0, 1, \cdots, M, \quad n = 0, 1, 2, \cdots$$

Let u_j^n, v_j^n and w_j^n be the approximations of $u(x_j, t_n)$, $v(x_j, t_n)$ and $w(x_j, t_n)$ respectively, and u^n, v^n and w^n be the solution vectors with component u_j^n, v_j^n and w_j^n respectively.

From time $t = t_n = nk$ to $t = t_{n+1} = t_n + k$, the system (2.4)-(2.9) is solved in two splitting steps. One solves the free Schrödinger system first

$$iu_t + \frac{1}{2}u_{xx} = 0, \quad iv_t + \frac{1}{2}v_{xx} = 0, \quad iw_t + \frac{1}{4}w_{xx} = 0 \qquad (2.11)$$

for the time step of length k, followed by solving the nonlinear ODE system

$$iu_t + \frac{\alpha}{2}v^*w + \gamma_1\left(\frac{1}{4}|u|^2 + \frac{1}{6}|v|^2 + \frac{1}{2}|w|^2\right)u + \frac{\gamma_1}{12}v^2u^* + \frac{\gamma_2}{4}|w|^2v + bu = 0, \quad (2.12)$$

$$iv_t + \frac{\alpha}{2}u^*w + \gamma_1\left(\frac{1}{4}|v|^2 + \frac{1}{6}|u|^2 + \frac{1}{2}|w|^2\right)v + \frac{\gamma_1}{12}u^2v^* + \frac{\gamma_2}{4}|w|^2u - bv = 0, \quad (2.13)$$

$$iw_t + \alpha uv + \gamma_1\left(\frac{1}{2}|w|^2 + |u|^2 + |v|^2\right)w + \frac{\gamma_2}{2}(uv^* + u^*v)w - \frac{q}{2}w = 0, \quad (2.14)$$

for the same time step. The system (2.11) will be discretized in space by the Fourier spectral method and integrated in time *exactly* [3–6, 18]. For the nonlinear ODE system (2.12)-(2.14), we first rewrite it in the form

$$i\frac{\partial}{\partial t}\begin{pmatrix} u \\ v \\ w \end{pmatrix} + A(u, v, w)\begin{pmatrix} u \\ v \\ w \end{pmatrix} = 0, \qquad t_n \le t \le t_{n+1}, \qquad (2.15)$$

where

$$A = \begin{pmatrix} \gamma_1\left(\frac{1}{4}|u|^2 + \frac{1}{6}|v|^2 + \frac{1}{2}|w|^2\right) + b & \frac{1}{12}\gamma_1 u^*v - \frac{1}{4}\gamma_2|w|^2 & \frac{1}{2}\gamma_2 w^*v + \frac{\alpha}{2}v^* \\ \frac{1}{12}\gamma_1 uv^* - \frac{1}{4}\gamma_2|w|^2 & \gamma_1\left(\frac{1}{4}|v|^2 + \frac{1}{6}|u|^2 + \frac{1}{2}|w|^2\right) - b & \frac{1}{2}\gamma_2 w^*u + \frac{\alpha}{2}u^* \\ \frac{1}{2}\gamma_2 wv^* + \frac{\alpha}{2}v & \frac{1}{2}\gamma_2 wu^* + \frac{\alpha}{2}u & \gamma_1\left(\frac{1}{2}|w|^2 + |u|^2 + |v|^2\right) - \frac{1}{2}q \end{pmatrix},$$

with the coefficient matrix $A(u, v, w)$ a Hermitian matrix. Denote $\Phi = (u, v, w)^T$. Integrate (2.15) over the time interval $[t_n, t_{n+1}]$, approximate the integral by the trapezoidal quadrature [7], we get

$$\begin{aligned} \Phi(t_{n+1}) &= e^{i\int_{t_n}^{t_{n+1}} A(\Phi(\tau))\, d\tau}\Phi(t_n) \approx e^{i\frac{k}{2}[A(\Phi(t_n)) + A(\Phi(t_{n+1}))]}\Phi(t_n) \\ &\approx e^{i\frac{k}{2}[A(\Phi^n) + A(\Phi^{(1)})]}\Phi(t_n) := e^{ikB(\Phi^n)}\Phi(t_n), \end{aligned} \qquad (2.16)$$

where $\Phi^n := \Phi(t_n)$ and $\Phi^{(1)}$ is an approximation of $\Phi(t_{n+1})$ and can be computed from the ODE system (2.15) by any explicit method. Here we use the forward Euler method

to compute it as:

$$\Phi^{(1)} = \Phi^n + ikA(\Phi^n)\Phi^n,$$

$$B(\Phi^n) = \frac{1}{2}[A(\Phi^n) + A(\Phi^{(1)})].$$

Since $A(\Phi^n)$ is a Hermitian matrix, i.e. $(A^*(\Phi^n))^T = A(\Phi^n)$, thus $B(\Phi^n)$ is also a Hermitian matrix. Therefore, we can find a unitary matrix $P(\Phi^n)$ with $P^{-1}(\Phi^n) = (P^*(\Phi^n))^T$ and a real diagonal matrix $\Lambda(\Phi^n)$ such that

$$B(\Phi^n) = P(\Phi^n)\Lambda(\Phi^n)P^{-1}(\Phi^n) = P(\Phi^n)\Lambda(\Phi^n)(P^*(\Phi^n))^T. \tag{2.17}$$

Thus we can compute one-step approximation of the ODE system (2.15) as

$$\Phi^{n+1} = P(\Phi^n)\,e^{ik\Lambda(\Phi^n)}\,(P^*(\Phi^n))^T\,\Phi^n. \tag{2.18}$$

From time $t = t_n$ to $t = t_{n+1} = t_n + k$, we combine the splitting steps via the standard second-order Strang splitting [17]:

$$u_j^{(1)} = \frac{1}{M}\sum_{l=-M/2}^{M/2-1}\exp(-ik\mu_l^2/4)\,(\widehat{u^n})_l\,\exp(i\mu_l(x_j - a)),$$

$$v_j^{(1)} = \frac{1}{M}\sum_{l=-M/2}^{M/2-1}\exp(-ik\mu_l^2/4)\,(\widehat{v^n})_l\,\exp(i\mu_l(x_j - a)),$$

$$w_j^{(1)} = \frac{1}{M}\sum_{l=-M/2}^{M/2-1}\exp(-ik\mu_l^2/8)\,(\widehat{w^n})_l\,\exp(i\mu_l(x_j - a)),$$

$$\begin{pmatrix} u_j^{(2)} \\ v_j^{(2)} \\ w_j^{(2)} \end{pmatrix} = P(\Phi_j^{(1)})\,e^{ik\Lambda(\Phi_j^{(1)})}\,(P^*(\Phi_j^{(1)}))^T \begin{pmatrix} u_j^{(1)} \\ v_j^{(1)} \\ w_j^{(1)} \end{pmatrix}, \qquad j = 0, 1, \cdots, M - 1,$$

$$u_j^{n+1} = \frac{1}{M}\sum_{l=-M/2}^{M/2-1}\exp(-ik\mu_l^2/4)\,(\widehat{u^{(2)}})_l\,\exp(i\mu_l(x_j - a)),$$

$$v_j^{n+1} = \frac{1}{M}\sum_{l=-M/2}^{M/2-1}\exp(-ik\mu_l^2/4)\,(\widehat{v^{(2)}})_l\,\exp(i\mu_l(x_j - a)),$$

$$w_j^{n+1} = \frac{1}{M}\sum_{l=-M/2}^{M/2-1}\exp(-ik\mu_l^2/8)\,(\widehat{w^{(2)}})_l\,\exp(i\mu_l(x_j - a)), \tag{2.19}$$

where $\Phi_j^{(1)} = (u_j^{(1)}, v_j^{(1)}, v_j^{(1)})^T$ $(j = 0, 1, \cdots, M)$, and $\hat{f}_l$, the Fourier coefficients of $f = (f_0, f_1, \cdots, f_M)^T$ with $f_0 = f_M$, are defined as

$$\mu_l = \frac{2\pi l}{b - a}, \qquad \hat{f}_l = \sum_{j=0}^{M-1} f_j \, \exp(-i\mu_l(x_j - a)), \quad l = -\frac{M}{2}, \cdots, \frac{M}{2} - 1.$$

Remark 2.1. If the decomposition of the Hermitian matrix $B(\Phi^n)$ in (2.17) couldn't be done explicitly, one can do it numerically, i.e. compute the eigenvalues and eigenvectors numerically, since it is only a 3×3 matrix.

3 Properties of the scheme and accuracy test

In this section, we will demonstrate the properties of our discretization (2.19) and test the spatial/temporal accuracy numerically.

3.1 Properties of the scheme

First, the discretization (2.19) for the system (2.4)-(2.9) is explicit and time reversible, i.e. the scheme is unchanged if we interchange $n \longleftrightarrow n + 1$ and $k \longleftrightarrow -k$ in it.

Second, another main advantage of the time-splitting method (2.19) is that it is time transverse invariant, just as for the original system (2.1)-(2.3) itself. If the constants α_1, α_2 are added to the potentials b and q respectively, then the discrete wave functions u_j^{n+1}, v_j^{n+1} and w_j^{n+1} obtained from (2.19) get multiplied by the phase factors $e^{i\alpha_1(n+1)k}$, $e^{-i\alpha_1(n+1)k}$ and $e^{-i\alpha_2(n+1)k/2}$ respectively, which leaves the amplitudes of the wave functions $|u_j^{n+1}|$, $|v_j^{n+1}|$ and $|w_j^{n+1}|$ unchanged. This property does not hold for the Crank-Nicolson finite difference method [15] and the leap-frog spectral method [12] for the system.

Third, the disretization (2.19) is unconditionally stable and conserves the total energy E in (2.10) in the discretized level, i.e. we have the following lemma

Lemma 3.1. *The time-splitting spectral scheme* (2.19) *is unconditionally stable. In fact, under any mesh size h and time step k, we have*

$$E^{n+1} := \|u^{n+1}\|^2 + \|v^{n+1}\|^2 + \|w^{n+1}\|^2 \equiv \|u_0\|^2 + \|v_0\|^2 + \|w_0\|^2$$

$$:= \frac{b-a}{M} \sum_{j=0}^{M} \left[|u_0(x_j)|^2 + |v_0(x_j)|^2 + |w_0(x_j)|^2 \right], \quad n = 0, 1, \cdots, \qquad (3.1)$$

where $\| \cdot \|$ is the discrete l^2-norm of a vector defined as

$$\|u^n\|^2 := \frac{b-a}{M} \sum_{j=0}^{M-1} |u_j^n|^2. \qquad (3.2)$$

Proof.　　For the scheme (2.19), by the Pasaval equality, we have

$$\frac{M}{b-a}E^{n+1}$$

$$:= \sum_{j=0}^{M-1}\left[|u_j^{n+1}|^2+|v_j^{n+1}|^2+|w_j^{n+1}|^2\right]=\frac{1}{M}\sum_{l=-M/2}^{M/2-1}\left[|(\widehat{u^{(2)}})_l|^2+|(\widehat{v^{(2)}})_l|^2+|(\widehat{w^{(2)}})_l|^2\right]$$

$$= \sum_{j=0}^{M-1}\left[|u_j^{(2)}|^2+|v_j^{(2)}|^2+|w_j^{(2)}|^2\right]=\sum_{j=0}^{M-1}((\Phi^{(2)})^*)^T\,\Phi^{(2)}$$

$$= \sum_{j=0}^{M-1}((\Phi^{(1)}))^*)^T P(\Phi_j^{(1)})e^{-ik\Lambda(\Phi_j^{(1)})}(P^*(\Phi_j^{(1)}))^T P(\Phi_j^{(1)})\,e^{ik\Lambda(\Phi_j^{(1)})}\,(P^*(\Phi_j^{(1)}))^T\,\Phi^{(1)}$$

$$= \sum_{j=0}^{M-1}((\Phi^{(1)})^*)^T\,\Phi^{(1)}=\sum_{j=0}^{M-1}\left[|u_j^{(1)}|^2+|v_j^{(1)}|^2+|w_j^{(1)}|^2\right]$$

$$= \sum_{j=0}^{M-1}\left[|u_j^n|^2+|v_j^n|^2+|w_j^n|^2\right]=\frac{M}{b-a}E^n,\qquad n\geq 0. \tag{3.3}$$

Thus the desired equality (3.1) is obtained from (3.3) by induction.　　　　□

3.2　Accuracy test

In order to test the spatial/temporal accuracy of the TSSP method (2.19), we solve the problem on the interval $[-16,16]$ with $\alpha=1$, $\gamma_1=1$, $\gamma_2=\frac{1}{6}$ and $b=q=0$. The initial data in (2.7) is taken as

$$u_0(x)=\frac{3}{2}\operatorname{sech}^2\frac{\sqrt{2}x}{2},\qquad v_0(x)=u_0(x),\qquad w_0(x)=0,\qquad x\in\mathbb{R}.$$

Let u, v and w be the 'exact' solutions which are obtained numerically by using our numerical method with a very fine mesh and time step, e.g. $h=1/64$ and $k=1/16384$, and $u^{h,k}$, $v^{h,k}$ and $w^{h,k}$ be the numerical solutions obtained by using our method with mesh size h and time step k. Fig. 1 plots the amplitudes, i.e. $|u|$ and $|w|$ of the solutions u and w. To quantify the numerical method, we define the error function as

$$e(t):=\sqrt{\frac{||u(\cdot,t)-u^{h,k}(\cdot,t)||^2+||v(\cdot,t)-v^{h,k}(\cdot,t)||^2+||w(\cdot,t)-w^{h,k}(\cdot,t)||^2}{||u(\cdot,t)||^2+||v(\cdot,t)||^2+||w(\cdot,t)||^2}},$$

where $\|\cdot\|$ is the standard l^2-norm as defined in (3.2).

　　First, we test the discretization error in space. In order to do this, we choose a very small time step, e.g. $k=1/16384$, such that the error from time discretization is negligible compared with the spatial disretization error. Table 1 lists the numerical error $e(t)$ at $t=1$
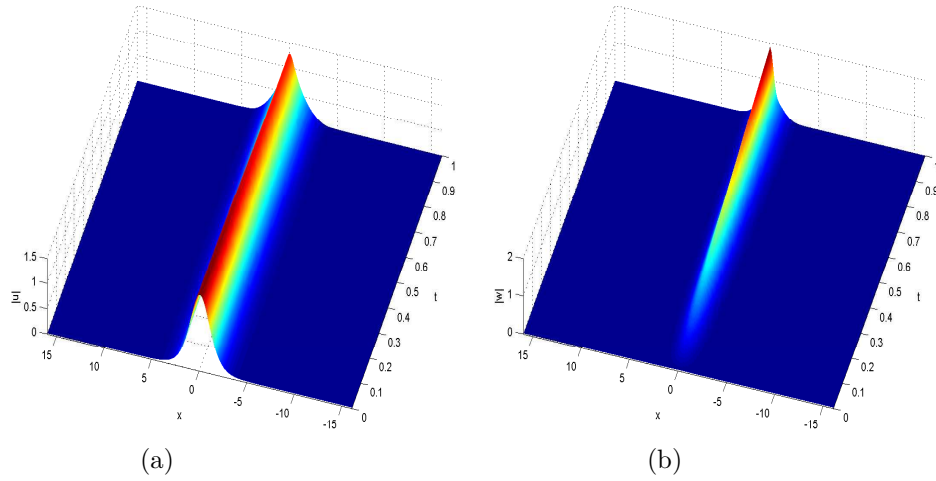
Table 1: Spatial discretization error analysis: at time $t = 1.0$ under $k = 1/16384$.

Spatial mesh size	$h = 1/2$	$h = 1/4$	$h = 1/8$	$h = 1/16$
$e(t = 1.0)$	2.537E-2	2.329E-4	2.283E-8	3.255E-12
Convergence order	-	6.767	13.32	12.77

Table 2: Temporal discretization error analysis: at time $t = 1.0$ under $h = 1/64$.

Time step size	$k = 1/128$	$k = 1/256$	$k = 1/512$	$k = 1/1024$
$e(t = 1.0)$	6.806E-5	1.702E-5	4.252E-6	1.060E-6
Convergence order	-	2.000	2.001	2.004

(a)   (b)

Figure 1: Time evolution of the solutions. (a) $|u|$; (b) $|w|$.

with different mesh sizes h. Second, we test the discretization error in time. Table 2 shows the numerical error $e(t)$ at $t = 1.0$ under different time steps k with mesh size $h = 1/64$. In addition, Fig. 2 plots the total wave energy $E(t)$.

From Tables 1 and 2, we can see that our TSSP method (2.19) is second order accurate in time and spectral order accurate in space. Furthermore, Fig. 2 demonstrates that our scheme conserves the total wave energy $E(t)$ *exactly* in the discretized level.

4 Three-wave dynamics and interactions

In this section, we apply our efficient and accurate method (2.19) to study the dynamics and interaction of three-waves in nonlinear optics modeled by the system (2.1)-(2.3).
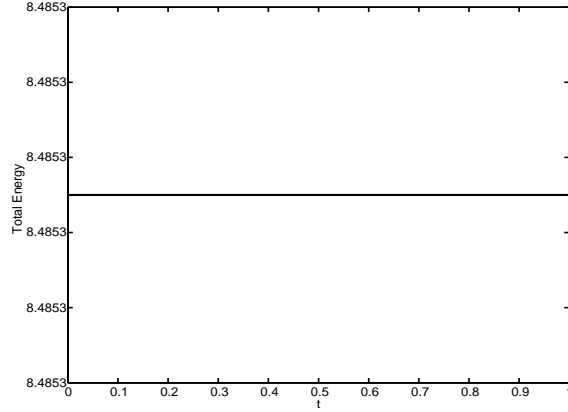
Figure 2: Conservation of the total wave energy $E(t)$.

4.1　Results in 1D

For the system (2.1)-(2.3) in 1D, if we set $v = w = 0$ in (2.1), resp. $u = w = 0$ in (2.2) and $u = v = 0$ in (2.3), it is reduced to three independent nonlinear Schrödinger equation with cubic nonlinearity. When $\gamma_1 > 0$, they admit the following solitary solutions:

$$u_s(x,t) = 2\sqrt{\frac{\beta_1}{\gamma_1}}\, \text{sech}\left(\sqrt{\beta_1}\left(x - \frac{c_1 t}{2}\right)\right) e^{i\left(\frac{c_1}{2}x + (\frac{\beta_1}{2} + b - \frac{c_1^2}{8})t\right)},\tag{4.1}$$

$$v_s(x,t) = 2\sqrt{\frac{\beta_2}{\gamma_1}}\, \text{sech}\left(\sqrt{\beta_2}\left(x - \frac{c_2 t}{2}\right)\right) e^{i\left(\frac{c_2}{2}x + (\frac{\beta_2}{2} - b - \frac{c_2^2}{8})t\right)},\ x \in \mathbb{R},\ t \geq 0,\tag{4.2}$$

$$w_s(x,t) = 2\sqrt{\frac{\beta_3}{\gamma_1}}\, \text{sech}\left(2\sqrt{\beta_3}\left(x - \frac{c_3 t}{4}\right)\right) e^{i\left(\frac{c_3}{2}x + (\beta_3 - \frac{c_3^2}{16})t\right)},\tag{4.3}$$

where β_j $(j = 1, 2, 3)$ are the amplitudes and c_j $(j = 1, 2, 3)$ are the velocities.

In order to study three-wave interactions in 1D, we choose the initial data in (2.7) for (2.1)-(2.3) as

$$u_0(x) = u_s(x - x_0, t = 0), \qquad v_0(x) = v_s(x - x_1, t = 0),$$
$$w_0(x) = w_s(x - x_2, t = 0), \qquad x \in \mathbb{R}.\tag{4.4}$$

and study three cases with $\alpha = 1$, $\gamma_1 = 8$ and $\gamma_2 = 4/3$:

Case I. Interaction of three stationary solitons, i.e. we choose $\beta_1 = \beta_2 = \beta_3 = 2$, $c_1 = c_2 = c_3 = 0$, $x_0 = -2.5$, $x_1 = 2.5$ and $x_2 = 0$ in (4.1)-(4.4).

Case II. Interaction of two fundamental solitons with a second harmonic stationary soliton, i.e. we choose $\beta_1 = \beta_2 = \beta_3 = 2$, $c_1 = c_2 = 2\sqrt{2}$, $c_3 = 0$, $x_0 = -8$, $x_1 = 8$ and $x_2 = 0$ in (4.1)-(4.4).

Case III. Interaction of two fundamental solitons, i.e. we choose $\beta_1 = \beta_2 = 2$, $\beta_3 = 0$, $c_1 = c_2 = 2$, $c_3 = 0$, $x_0 = -8$, $x_1 = 8$ and $x_2 = 0$ in (4.1)-(4.4).

We solve the problem on $[-16, 16]$ with mesh size $h = 1/128$ and time step $k = 0.0001$. Figs. 3 and 4 show time evolution of the solutions $|u|$, $|v|$ and $|w|$, and wave energies respectively, for Case I with different parameters b and q. Figs. 5 and 6 show similar results for Case II, and Figs. 7 and 8 for Case III.

From Figs. 3-8, we can draw the following conclusions: (i) Due to the soliton-type initial data, if the solutions of different waves are well-separated, they will propagate themselves without interaction (cf. Figs. 5 and 7 before $t = 4$) and the wave energy of each wave is conserved (cf. Figs. 6 and 8 before $t = 4$). (ii) Interactions are observed when the solutions of different waves are overlapped (cf. Figs. 3, 5 and 7) and wave energies of different waves are exchanged (cf. Figs. 4, 6 and 8). (iii) Symmetric property of the three waves are kept during the interaction when $b = q = 0$, while conspicuous emission of acoustic waves and inconspicuous emission of sound waves are observed when either $b \neq 0$ or $q \neq 0$. (iv) The total wave energy is conserved in all the cases which confirm the results in Lemma 3.1.

Furthermore, we also study the influence of the cubic nonlinearities. In fact, when $\alpha = 1$, $\gamma_1 = \gamma_2 = b = 0$, the system (1.1)-(1.3) in 1D admits a stationary vectorial soliton solution

$$u_v(x,t) = v_v(x,t) = \frac{3k}{2} \operatorname{sech}^2 \left(\frac{\sqrt{2k}x}{2} \right) e^{ikt}, \tag{4.5}$$

$$w_v(x,t) = 3k \operatorname{sech}^2 \left(\frac{\sqrt{2k}x}{2} \right) e^{2ikt}, \qquad x \in \mathbb{R}, \quad t \geq 0, \tag{4.6}$$

with $q = -3k$. We solve the problem (2.1)-(2.3) in 1D on $[-16, 16]$ with mesh size $h = 1/128$ and time step $k = 0.0001$. The initial data is chosen as

$$u_0(x) = v_0(x) = u_v(x, t = 0), \qquad w_0(x) = w_v(x, t = 0), \qquad x \in \mathbb{R}. \tag{4.7}$$

We choose the parameters $\alpha = 1$, $\gamma_1 = \gamma_2 = 0$ when time $t \leq 4$, and $\alpha = 1$, $\gamma_1 = 1$, $\gamma_2 = 1/6$ when $t > 4$. Thus the cubic nonlinearities are turned on at time $t = 4$. Figures 9 and 10 depict time evolution of the solutions $|u|$, $|v|$ and $|w|$, and wave energies respectively.

From Figs. 9 and 10, we can see that: (i) without the cubic nonlinearities, the amplitudes remain the same with time (cf. Fig. 9 before $t = 4$) and the wave energy of different waves is conserved (cf. Fig. 10 before $t = 4$); (ii) when the cubic nonlinearities are turned on, they have a focusing effect to the soliton, i.e. the solitons shrink and change to a breather, with part of the energy radiated (cf. Figs. 9 and 10 after $t = 4$).

4.2   Results in 2D

In this subsection, we simulate wave interactions of (2.1)-(2.3) in two transverse coordinates, i.e. we choose $\alpha = 1$, $\gamma_1 = 1$, $\gamma_2 = 1/6$, $b = 0$ and $q = 0$. The initial data is chosen
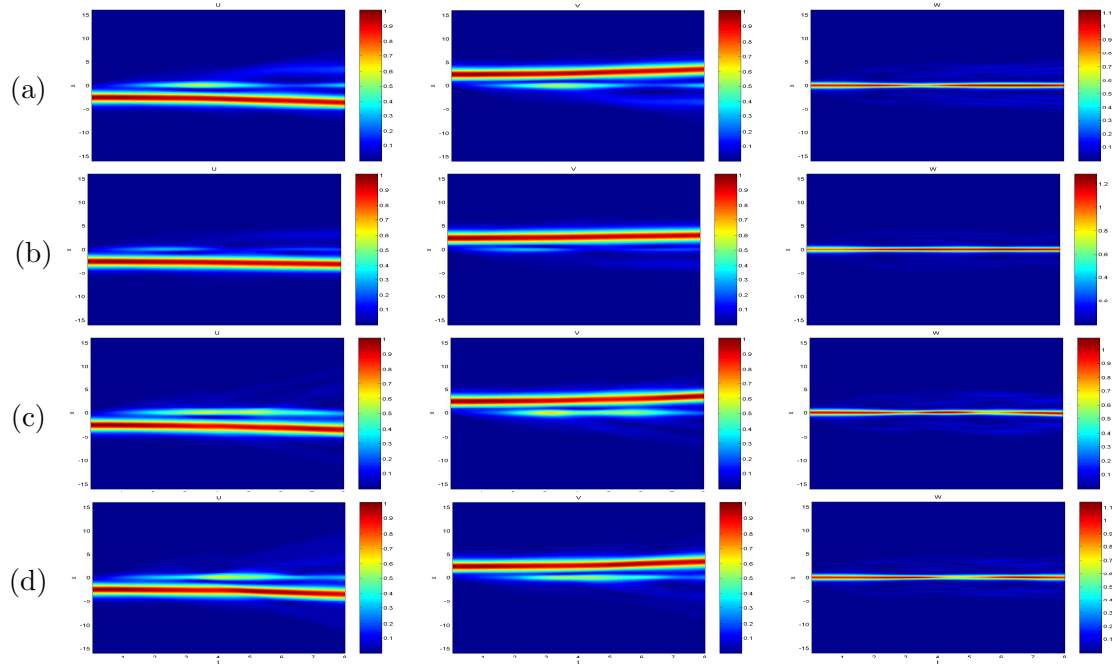
Figure 3: Time evolution of the solutions $|u|$, $|v|$ and $|w|$ for interaction of three stationary solitons, i.e. Case I. (a) $b = 0$, $q = 0$; (b) $b = 0$, $q = 1$; (c) $b = 1$, $q = 0$; and (d) $b = 1$, $q = 1$.
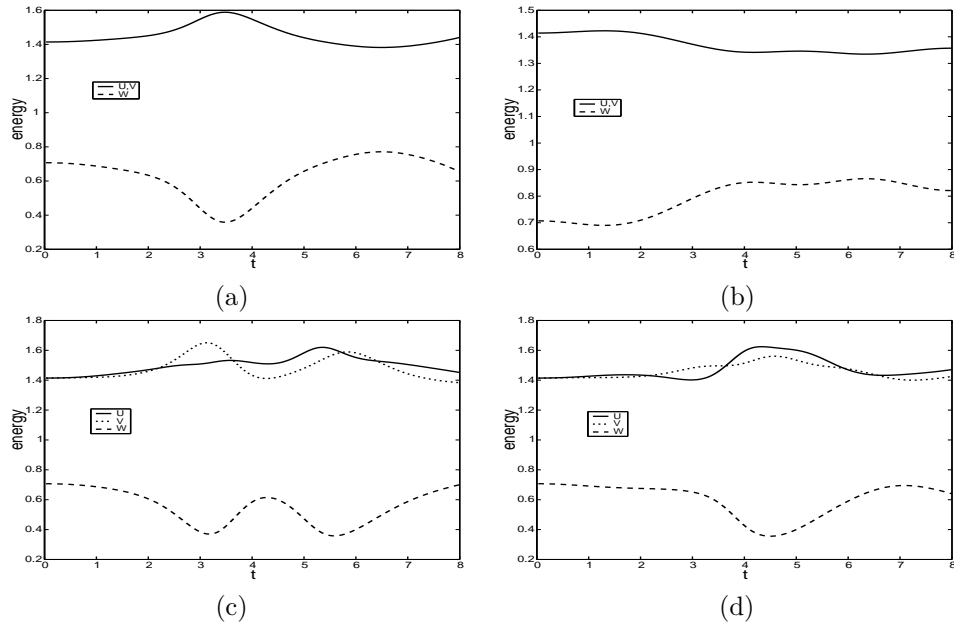

Figure 4: Time evolution of wave energies in Case I. (a) $b = 0$, $q = 0$; (b) $b = 0$, $q = 1$; (c) $b = 1$, $q = 0$; and (d) $b = 1$, $q = 1$.

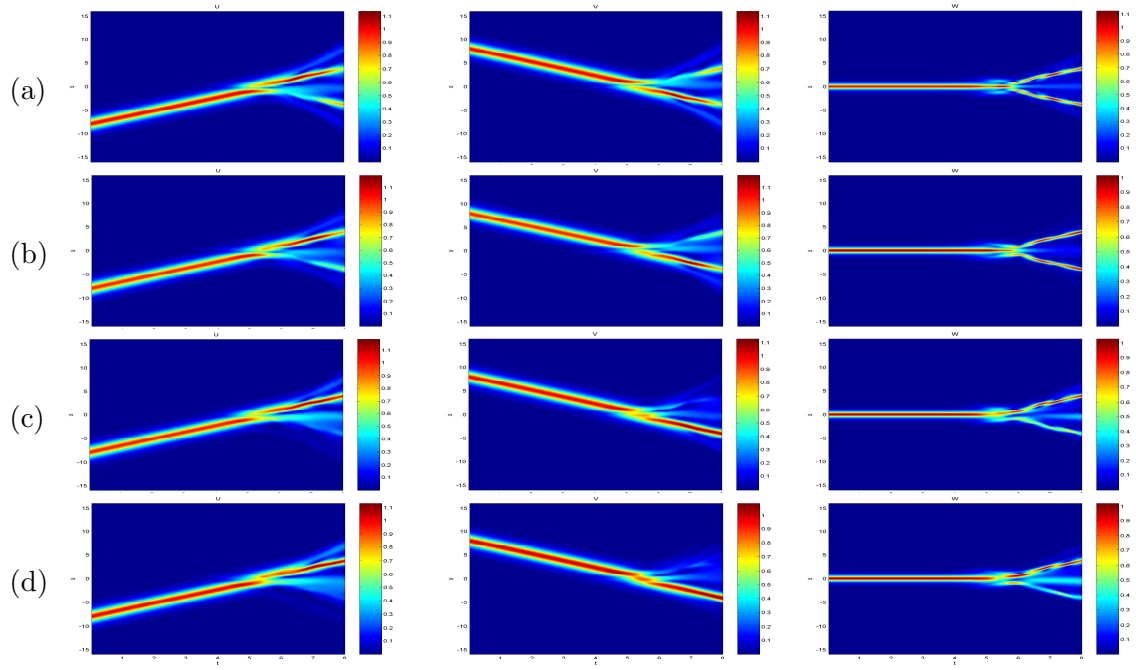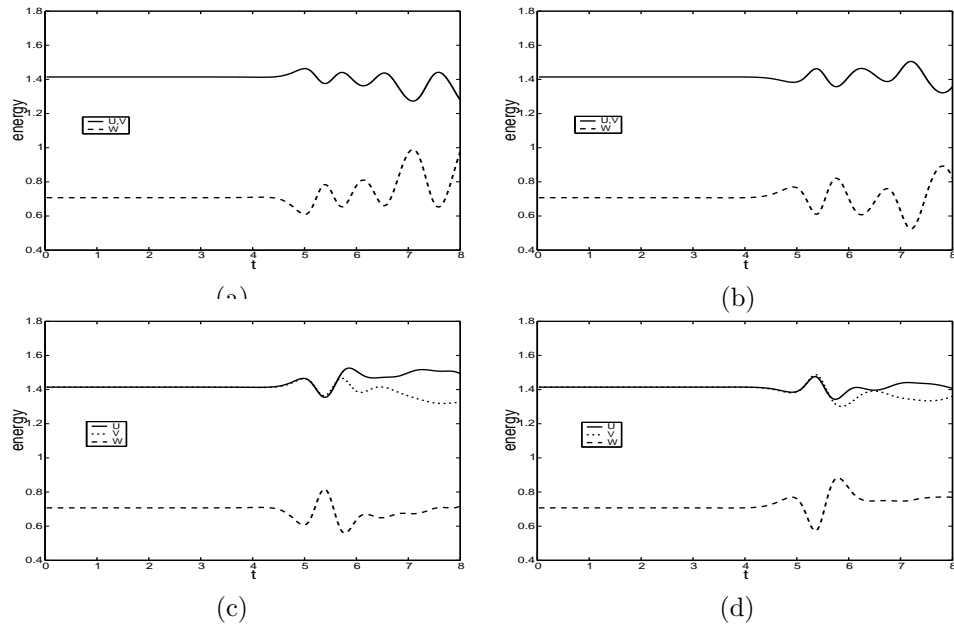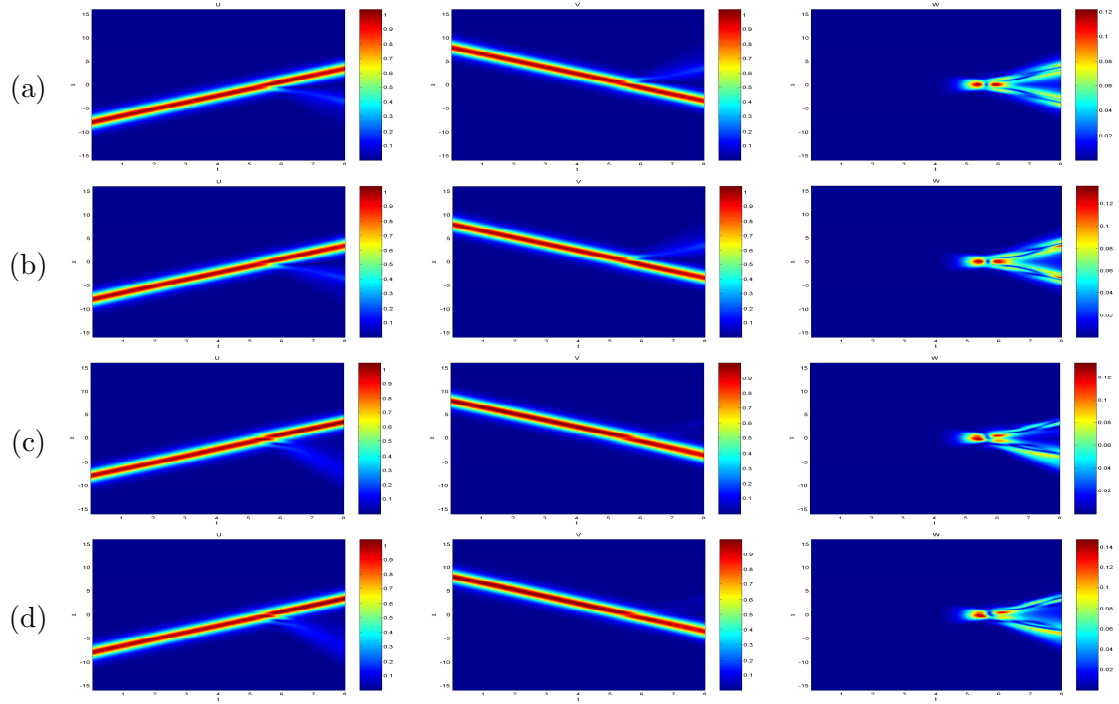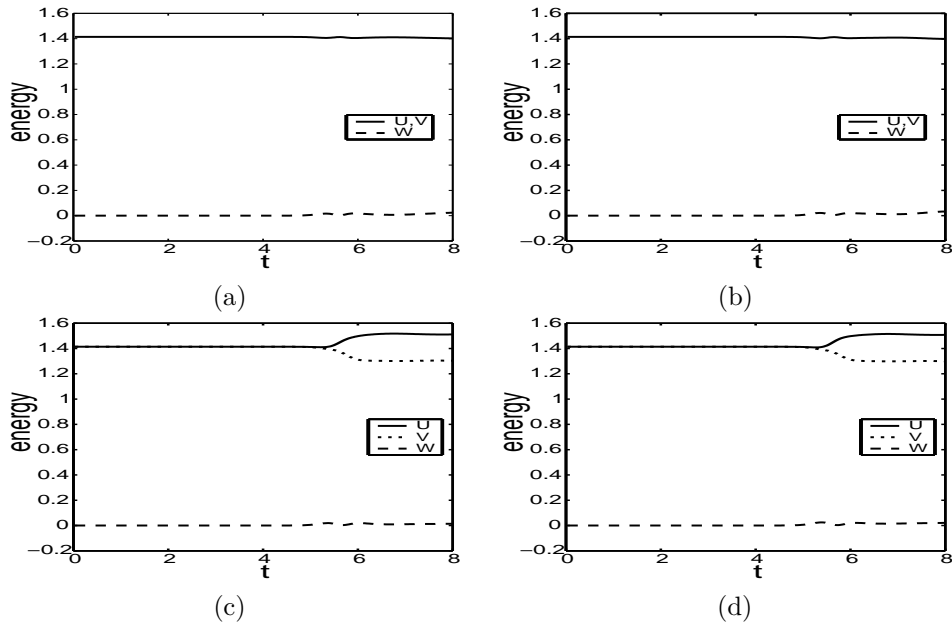Figure 5: Time evolution of the solutions $|u|$, $|v|$ and $|w|$ for interaction of two fundamental solitons with a second harmonic stationary soliton, i.e. Case II. (a) $b = 0$, $q = 0$; (b) $b = 0$, $q = 1$; (c) $b = 1$, $q = 0$; and (d) $b = 1$, $q = 1$.

Figure 6: Time evolution of wave energies in Case II. (a) $b = 0$, $q = 0$; (b) $b = 0$, $q = 1$; (c) $b = 1$, $q = 0$; and (d) $b = 1$, $q = 1$.
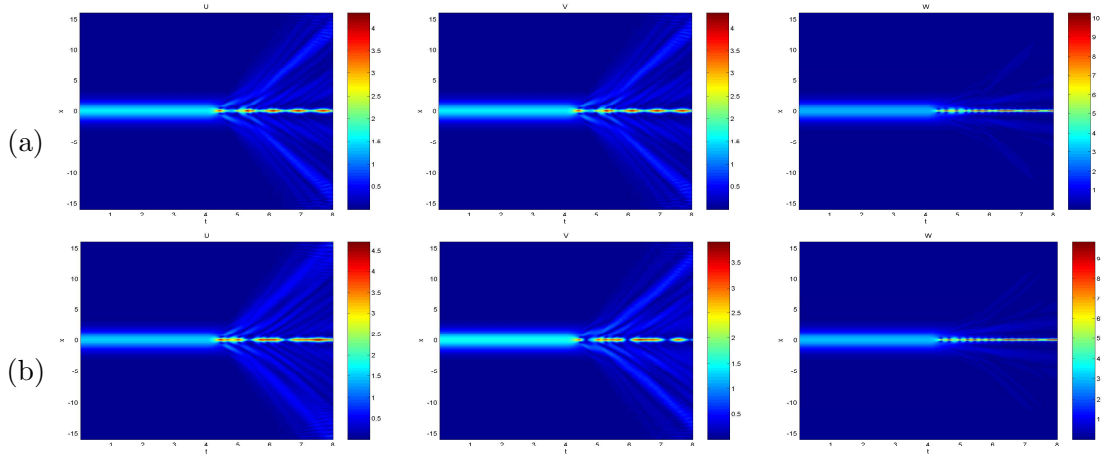
Figure 7: Time evolution of the solutions $|u|$, $|v|$ and $|w|$ for interaction of two fundamental solitons, i.e. Case III. (a) $b = 0$, $q = 0$; (b) $b = 0$, $q = 1$; (c) $b = 1$, $q = 0$; and (d) $b = 1$, $q = 1$.

Figure 8: Time evolution of wave energies in Case III. (a) $b = 0$, $q = 0$; (b) $b = 0$, $q = 1$; (c) $b = 1$, $q = 0$; and (d) $b = 1$, $q = 1$.

Figure 9: Time evolution of the solutions $|u|$, $|v|$ and $|w|$ for turning on cubic nonlinearities. (a) $b = 0$; (b) $b = 1$.

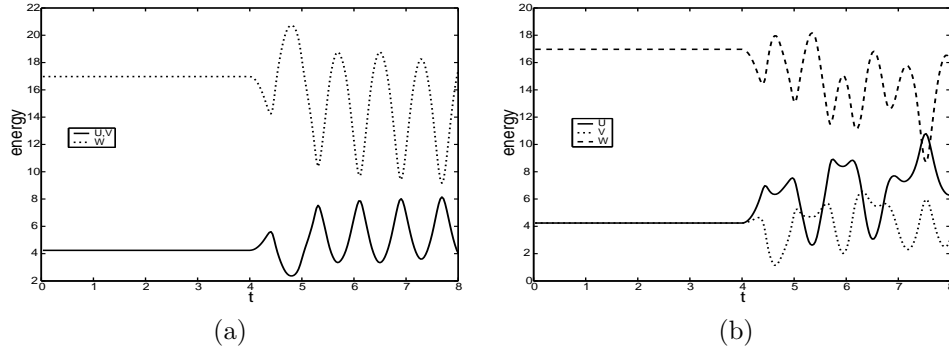Figure 10: Time evolution of wave energies for turning on cubic nonlinearities. (a) $b = 0$; (b) $b = 1$.

as

$$u_0(x, y) = v_0(x, y) = e^{-((x-1.5)^2 + y^2)} + e^{-((x+1.5)^2 + y^2)},$$
$$w_0(x, y) = 0, \qquad (x, y) \in \mathbb{R}^2. \tag{4.8}$$

We solve the problem on $[-16, 16] \times [-16, 16]$ with mesh size $h = \frac{1}{4}$ and time step $k = \frac{1}{32}$.

Fig. 11 shows the solutions $|u|$ and $|w|$ for different times and Fig. 12 depicts the wave energies of u and w.

From Figs. 11 and 12, we can see that a second harmonic wave is generated during their interaction (cf. Fig. 11), and with the time evolution, more and more energy is transfered from the fundamental waves to the second harmonic wave. Furthermore, the interaction of two Gaussian-type waves leads to the formation of another Gaussian-like wave packet at the center of the plane, it absorbs more and more wave energy and finally dominates the initial two Gaussian-type waves. This example also demonstrates the efficiency and high resolution of our numerical method.
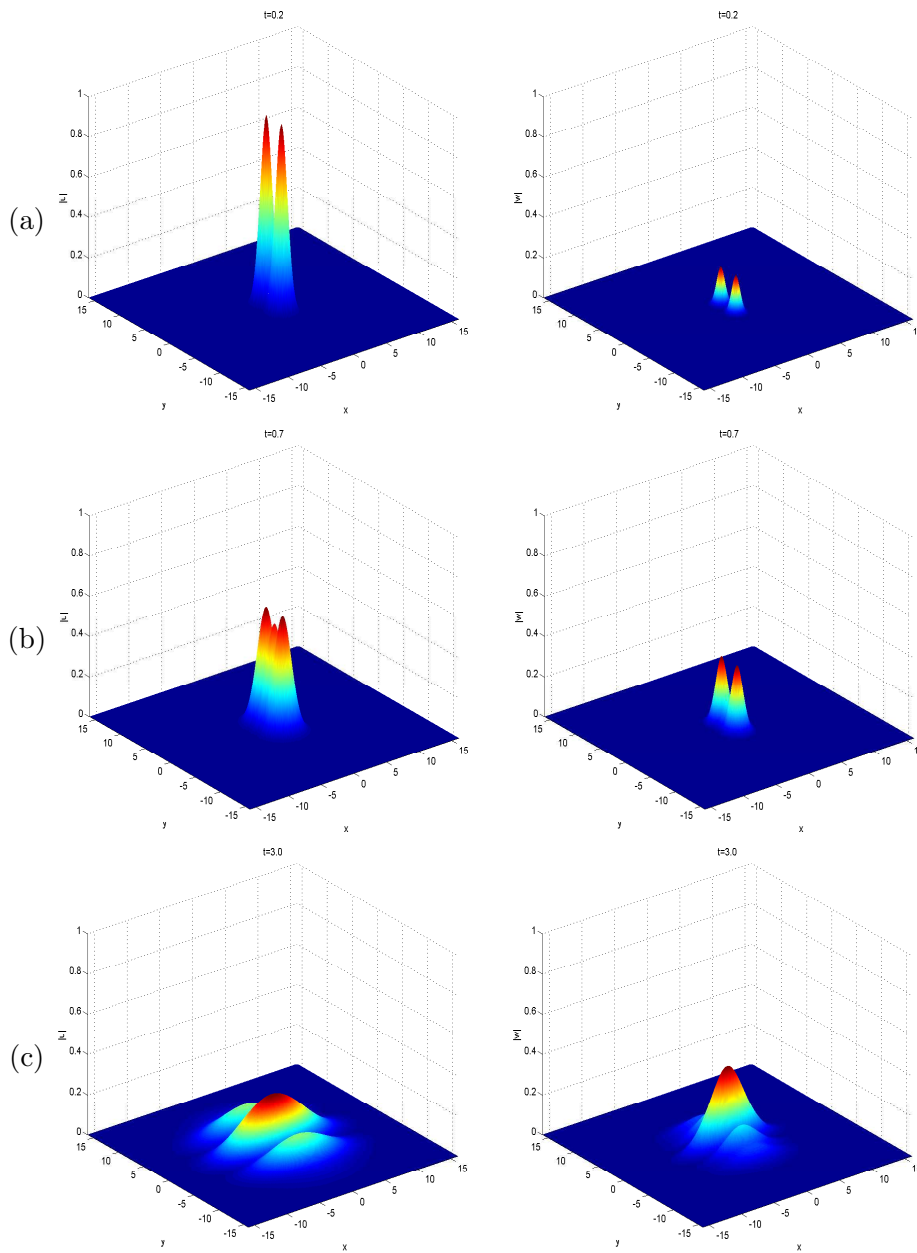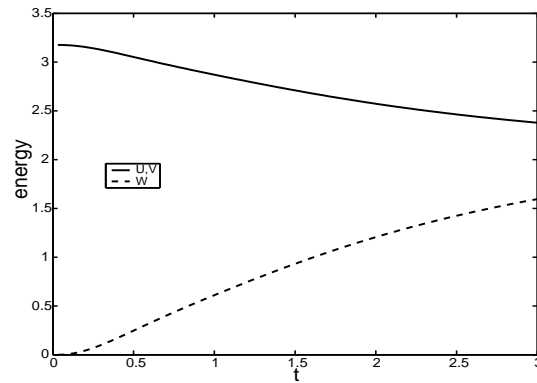
Figure 11: Surface plots of the solutions $|u|$ (left column) and $|w|$ (right column) at different times. (a) $t = 0.2$; (b) $t = 0.7$; and (c) $t = 3.0$.

5   Conclusion

An efficient and accurate time-splitting spectral (TSSP) method is designed for a general model of three-wave optical interactions arising from nonlinear optics with competing

Figure 12: Time evolution of wave energies of u and w.

quadratic and cubic nonlinearities by formulating the terms related to quadratic and cubic nonlinearities into a Hermitian matrix in a proper way. The method is explicit, unconditionally stable, time reversible, time transverse invariant, of spectral accuracy in space and second order accuracy in time. Furthermore, it conserves the total wave energy. We apply the novel numerical method to study three-wave interactions and observe different interaction patterns. Furthermore, the method is also applied to simulate wave interactions in two dimensions which is not studied in the literature yet.

Acknowledgments

References

[1] D. M. Baboiu and G. I. Stegeman, Solitary-wave interactions in quadratic media near type I phase-matching conditions, J. Opt. Soc. Am. B, 14 (1997), 3143-3150.
[2] D. M. Baboiu and G. I. Stegeman, Interaction of soliton-like light beams in second-order nonlinear materials, Opt. Quant. Electron, 30 (1998), 849-859.
[3] W. Bao and D. Jaksch, An explicit unconditionally stable numerical methods for solving damped nonlinear Schrodinger equations with a focusing nonlinearity, SIAM J. Numer. Anal., 41 (2003), 1406-1426.
[4] W. Bao, D. Jaksch and P. A. Markowich, Numerical solution of the Gross-Pitaevskii equation for Bose-Einstein condensation, J. Comput. Phys., 187 (2003), 318-342.
[5] W. Bao, S. Jin and P. A. Markowich, On time-splitting spectral approximations for the Schrödinger equation in the semiclassical regime, J. Comput. Phys., 175 (2002), 487-524.
[6] W. Bao, S. Jin and P. A. Markowich, Numerical study of time-splitting spectral discretizations of nonlinear Schrödinger equations in the semi-clasical regimes, SIAM J. Sci. Comp., 25 (2003), 27-64.

[7] W. Bao, P. A. Markowich, C. Schmeiser and R. M. Weishaupl, On the Gross-Pitaevskii equation with strongly anisotropic confinement: Formal asymptotics and numerical experiments, Math. Mod. Meth. Appl. Sci., 15 (2005), 767-782.

[8] C. Besse, B. Bidegaray and S. Descombes, Order estimates in time of splitting methods for the nonlinear Schrödinger equation, SIAM J. Numer. Anal., 40 (2002), 26-40.

[9] K. J. Blow, N. J. Doran and D. Wood, Polarization instabilities for solitons in birefringent fibers, Opt. Lett., 12 (1987), 202-204.

[10] K. J. Blow and D. Wood, The evolution of solitons from non-transform limited pulses, Opt. Commun., 58 (1986), 349-354.

[11] A. V. Buryak, P. D. Trapani, D. V. Skryabin and S. Trillo, Optical solitons due to quadratic nonlinearities: From basic physics to futuristic applications, Phys. Rep., 370 (2002), 63-235.

[12] M. Chen, D. J. Kaup and B. A. Malomed, Three-wave solitons and continuous waves in media with competing quadratic and cubic nonlinearities, Phys. Rev. E, 69 (2004), 056605.

[13] C. B. Clausen, O. Bang and Y. S. Kivshar, Spatial solitons and induced Kerr effects in quasi-phase-matched quadratic media, Phys. Rev. Lett., 78 (1997), 4749-4752.

[14] J. F. Corney and O. Bang, Solitons in quadratic nonlinear photonic crystals, Phys. Rev. E, 64 (2001), 047601.

[15] C. Etrich, U. Peschel, F. Lederer, B. A. Malomed and Y. S. Kivshar, Origin of the persistent oscillations of solitary waves in nonlinear quadratic media, Phys. Rev. E, 54 (1996), 4321-4324.

[16] R. Glowinski and P. L. Tallec, Augmented Lagrangians and Operator Splitting Methods in Nonlinear Mechanics, SIAM, Philadelphia, 1989.

[17] G. Strang, On the construction and comparison of difference schemes, SIAM J. Numer. Anal., 5 (1968), 506-517.

[18] T. R. Taha and M. J. Ablowitz, Analytical and numerical aspects of certain nonlinear evolution equations II: Numerical, nonlinear Schrödinger equation, J. Comput. Phys., 55 (1984), 203-230.

[19] J. Weideman and B. Herbst, Split-step methods for the solution of the nonlinear Schrödinger equation, SIAM J. Numer. Anal., 23 (1986), 485-507.